17th World Conference on Earthquake Engineering, 17WCEE
Sendai, Japan - September 13th to 18th 2020

Damage Investigation of Non-structural Components in Buildings with SHM System in the 2018 Osaka Earthquake

S. Ogasawara[1], K. Kanda[2], Y. Suzuki[3]

[1] *Structural Engineer, Kobori Research Complex Inc., saori-ogasawara@kobori-takken.co.jp*
[2] *Principal Researcher, Kobori Research Complex Inc., kandak@kobori-takken.co.jp*
[3] *General Manager, Kobori Research Complex Inc., y-suzuki@kobori-takken.co.jp*

Abstract

This paper reports the relationship between damage to non-structural components and the building response observed by sensors. We have installed a structural health monitoring ("SHM") system in about 400 buildings in Japan for five years to support emergency response such as evacuation judgment after an earthquake. Earthquakes have frequently occurred in various places in Japan, and seismic observation records of buildings with the SHM system have been accumulated. These records are useful for analyzing the actual behavior of buildings and the relationship between the building response and the damage caused by earthquakes. Therefore, we investigated damage states of the buildings installed the SHM system after the 2018 Osaka earthquake. The 2018 Osaka earthquake occurred at 7:58 am on June 18, 2018, whose epicenter was on the northern part of Osaka Prefecture. The magnitude of the earthquake was M_J 6.1 (M_W 5.5), and the depth of the epicenter was 13 km. The maximum seismic intensity 6-minus in JMA scale and more than 0.50g in PGA were observed in urban areas of Osaka Prefecture. Though there was almost no major damage to structural members of buildings, much damage was revealed to non-structural components. Therefore, we focused on the damage of non-structural components and analyzed by type of them. Since we had much damage data for interior walls and partition walls which tended to be damaged even in small interstory drift ratio, we tried to evaluate their fragility curve. In this way, if we obtain more actual damage data, we can evaluate fragility curve of the corresponding non-structural components accurately. As a result, it comes to improve the accuracy of damage judgement by SHM systems.

Keywords: structural health monitoring (SHM), non-structural components, damage, building response

1. Introduction

Numerous damages to non-structural components have been reported in past earthquakes. Damage to non-structural components commonly starts significantly earlier than that to major structural members and may be caused by more frequent medium magnitude earthquakes. The degree and cause of damage have been analyzed from damage surveys after the earthquake, and studies have been conducted to link the relationship between non-structural components damage and seismic intensity [1]. However, few analyzes the relationship between damage states and actual building response, because there was no observation record of buildings. Estimating the damage of not only structural members but also non-structural components from building response is useful in knowing the damage states of buildings.

After the 2011 Tohoku earthquake, the installation of SHM in buildings have been increasing in Japan. These are used by building owners and facility managers who are commonly not very familiar with structural engineering to ascertain safety or unsafety of a building immediately after an earthquake. We developed the SHM system called q-NAVIGATOR (nicknamed q-NAVI) in 2014 and this system has been installed in about 400 buildings as of December 2019. The installed buildings are located in urban areas throughout Japan, centered in large cities such as Tokyo and Osaka.

Of the earthquake ever observed by q-NAVI, in the 2018 Osaka Earthquake (June 18, 2018), large ground motion records (JMA Seismic Intensity 4 or more) were observed in multiple buildings. The post-earthquake investigation carried out by construction firms confirmed almost no major damage to structural members, but many non-structural components were damaged. Therefore, we investigated the damage of non-structural components of the buildings, analyzed the relationship between damage to non-structural components and building response, and examined the building response that caused damage to non-structural components.

2. Building observation and damage investigation in earthquakes

2.1 Structural health monitoring system : q-NAVI

The q-NAVI is a system that announces the state of buildings after an earthquake in three stages: “Safe”, “Caution”, or “Danger”. The standard system is shown in Figure 1, including multiple accelerographs (simply called sensors hereinafter) that measure the vibration of floors in the building, a PC for analysis, a monitor screen that displays the results, and an Uninterruptible Power Supply (UPS) for supplying power at the time of power loss. The sensor is adopted a mechanical capacitive accelerograph using a pendulum. The number of sensors to deploy for low- to mid-rise buildings is typically four, placing one tri-axial sensor (measuring two horizontal and one vertical directions) per few floors. The sensors are commonly installed on the floor slab.

The most important index to judge a building’s state is the maximum interstory drift ratio, but accelrographs can measure only accelerations. Hence, the maximum interstory drift ratio is calculated based on the displacements estimated by the double integration of the recorded accelerations.

2.2 Outline of the 2018 Osaka Earthquake

The 2018 Osaka Earthquake occurred at 7:58 am on June 18, 2018. Its epicenter was in the northern part of Osaka Prefecture. The magnitude of the earthquake was M_J 6.1 (M_W 5.5), and the depth of the epicenter was 13 km. The maximum JMA Seismic Intensity (I_{JMA}) of 6-minus was observed in urban areas of Osaka Prefecture. This intensity, I_{JMA}, is most commonly used in Japan as a scale of shaking amplitude. The human casualties were six, and 369 people were injured. The damaged houses included 18 collapses, 512 partial collapses, and 55,081 damaged without collapse.

Figure 2 shows a map of JMA Seismic Intensity values measured at the base floor of buildings by q-NAVI. The maximum JMA Seismic Intensity observed in the buildings was 5-plus, and many non-structural damages had been reported. So we discussed with the owners of those buildings, a damage survey was conducted on the 26 buildings in Osaka.

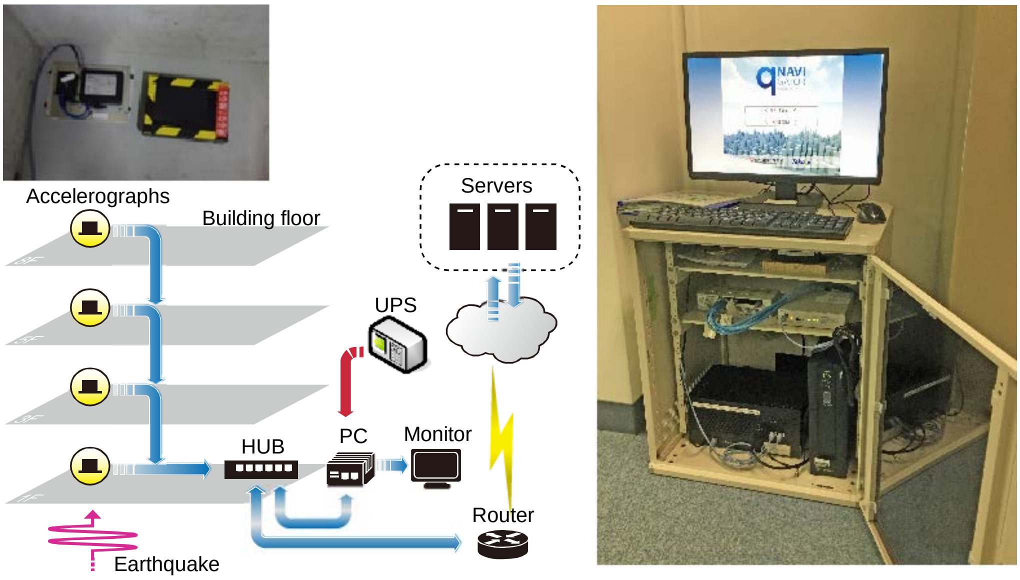

Fig. 1 – Outline of system configuration

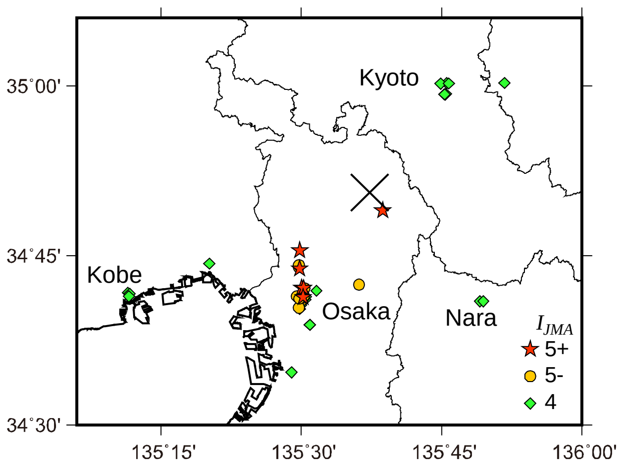

Fig. 2 – Map of JMA Seismic Intensity values measured at base floor of buildings, with a cross mark indicating epicenter

Table 1 – Non-structural components examined in survey

1	Exterior walls
2	Window glasses
3	Interior walls and partition walls
4	Doors
5	Ceilings
6	Furniture and building contents
7	Air conditioners and plumbing elements
8	Expansion joints

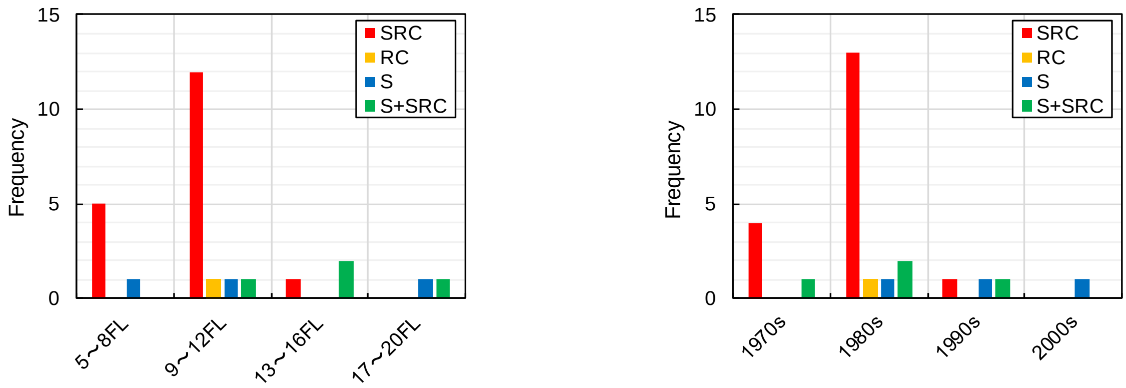

(a) (b)

Fig. 3 – Distributions of the 26 buildings in Osaka (SRC: steel encased reinforced concrete; RC: reinforced concrete; S: steel): (a) Distribution of number of stories; (b) Distribution of year of construction

2.3 Damage investigation of non-structural components

Figure 3 shows the number of stories and the year of construction of the 26 buildings. All of them are office buildings of seven to 20 stories in height, with the year of construction between 1974 and 2009. Composition with respect to the type of structure is 18 SRC (Steel Encased Reinforced Concrete) buildings, one RC building, three steel buildings and four combined steel and SRC buildings. Four of the SRC buildings were connected with expansion joints.

The damage investigation was conducted for eight types of non-structural components shown in Table 1. It was quantified primarily based on interviews with building managers carried out about two months after the earthquake. Some damage was already repaired, but in such cases, damage was confirmed by photos taken immediately after the earthquake.

3. Damage investigation of non-structural components

3.1 Observation records in the 2018 Osaka earthquake

We examined the observation records of the 26 buildings. Figure 4 shows the relationship between the maximum acceleration of the base floor and the maximum response (floor acceleration and interstory drift ratio), including plots for the two horizontal directions, based on the records observed by q-NAVI. Its floor accelerations at the base floor exhibited large in a range of 0.6 to 4.3 m/s^2. The estimated interstory drift ratios remained relatively small, in a range of 0.02 to 0.33% (1/5000 to 1/300). This was likely because the predominant period of ground motion was short (about 0.3 seconds), and the duration time was also short.

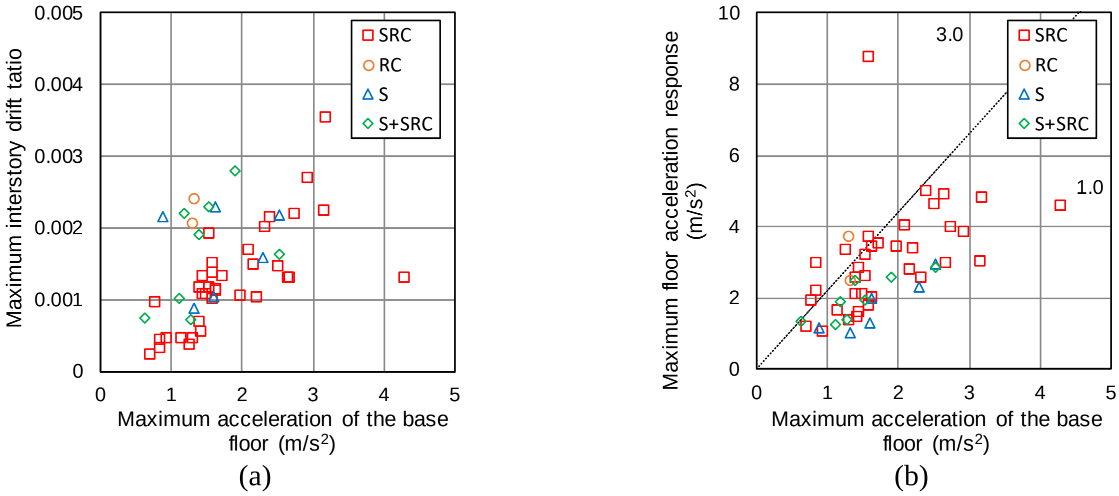

Fig. 4 – Relationship of response between base floor and floor sustaining maximum response: (a) Maximum interstory drift ratio; (b) Maximum floor acceleration

The maximum interstory drift ratio shown in Figure 4 (a) is at most 0.33% (1/300) and tends to increase as the base acceleration increases. For concrete-based buildings, the difference between the RC and SRC buildings occurred primarily because most SRC buildings have shear walls, while the RC building is made of moment frames that have fewer shear walls. The steel buildings and the combined steel and SRC buildings tend to be larger variation in the maximum interstory drift ratio because some buildings consist of only moment frames, while the rest are made of moment frames with braces.

The largest acceleration measured among all floors was 8.8 m/s^2 (0.90g), one significantly larger than the rest in Figure 4 (b). This particular record, was observed by a sensor near the damaged expansion joint, and most likely was obtained as a result of pulse-like vibration during its serious failure. Excluding this record, the maximum floor acceleration is in a range of 5.0 m/s^2 (0.50g). Figures 4 (b) also indicates that the floor acceleration is amplified by a factor of one to three from the base to the top. The maximum accelerations of most buildings exceeded 1.0 m/s^2 (0.10g), which has been confirmed as the approximate magnitude at which damage to non-structural components began to occur, particularly in ceilings, from the experience of the 2011 Tohoku earthquake [2].

3.2 Damage ratio of non-structural components

We investigated damage of non-structural components of the buildings. Figure 5 shows the damage ratio with respect to the number of buildings that sustained relevant damage. Here, the building is classified as damaged unless it did not exhibit any damage to the relevant non-structural components. Major characteristics observed from the survey are summarized as: 1) Most non-structural components around the expansion joints were damaged; 2) Many buildings suffered damage to interior walls, partition walls, and ceilings; 3) There was no damage to window glasses, doors, and furniture and building contents; and 4) Four buildings out of 26 (i.e., 15%) suffered no damage to non-structural components.

3.3 The relationship between damage to non-structural components and building response

Among the eight types of non-structural components, damage to exterior walls, window glasses, interior walls, partition walls, and doors depends primarily on the interstory drift ratio; hence the relationship between the maximum interstory drift ratio and the damage severity is of primary interest. On the other hand, damage to ceilings, furniture, and building contents is more sensitive to the acceleration; hence the relationship between the maximum acceleration at the corresponding floor and the damage severity is most relevant.

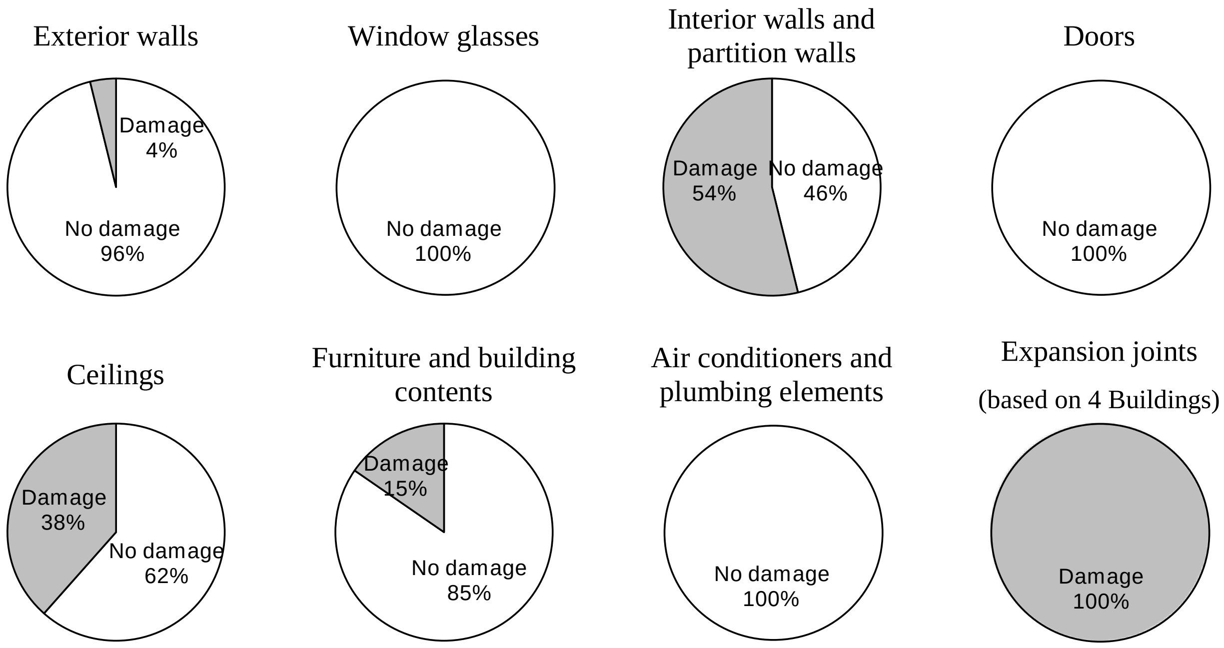

Fig. 5 – Damage ratio of non-structural components (based on 26 buildings)

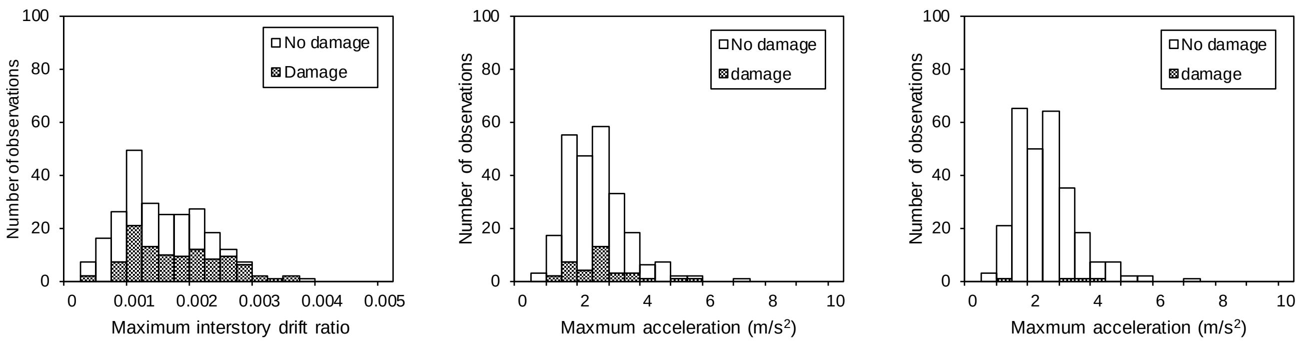

(a) Interior and partition walls (b) Ceilings (c) Furniture and building contents

Fig. 6 – Distributions of damage: (a) With respect to maximum interstory drift ratio; (b)(c) With respect to maximum floor acceleration

Figure 6 shows the maximum response (interstory drift ratio and floor acceleration) and the number of damage cases. Here the number of observations was classified as damaged when damage was observed in at least one non-structural component in the floor. The number was counted with respect to the floor of the section installed the sensor. The interstory drift ratio on each floor was the same in the section installed the sensor, and the acceleration on each floor was linearly interpolated in the section. Detailed investigation result of damaged components is presented below.

The survey of exterior walls was conducted for four types, tile cladding, stone cladding, ALC and curtain wall, which were often used in the buildings. One crack was observed at the corner of stone cladding wall, but no damage was reported on the other wall, such as falling tiles. The stone cladding wall was locally damaged at 0.19% (1/520) only, but the tile cladding wall was not damaged up to 0.24% (1/420). On the indoor side, cracks were observed on the concrete wall, which was the foundation for tile and stone cladding, and water leakage was also reported, so it was probable that the cracks occurred at the exterior walls. On the other hand, both ALC and curtain walls were not damaged up to about 0.36% (1/280).

Many small cracks occurred in interior and partition walls. Cracks were detected most extensively around core spaces running vertically, such as staircases and elevator shafts, and also around openings, such as doors and windows. Most of them were slight damage, characterized by fine cracks in the walls. Interior and partition walls were composed of many types of materials and installation methods, hence detailed classification of the walls was difficult. Therefore, the relationship between the maximum interstory drift ratio (of the two horizontal directions) and the damage severity of walls was analyzed without detailed classification into respective types of wall. Figure 6 (a) shows the maximum interstory drift ratio and the number of damage cases. In one case, cracks were observed at 0.05% (1/2000) in a concrete non-structural wall at the stair room, but most likely this occurred as a result of the concentration of local deformations in the wall. If this case is excluded, notable damage, i.e., cracks, was found to occur from a maximum interstory drift ratio of about 0.1% (1/1000).

As for the damage to ceilings, misalignment of ceiling panels and damage to lights and other equipment attached to the ceiling were observed most frequently. A few ceiling panels fell, where the maximum acceleration at the corresponding floor was 3.8 m/s^2 (0.39g). This was caused by collisions between the wall and ceiling. Figure 6 (b) shows the maximum acceleration at the corresponding floor and the number of damage cases that match the definition adopted for ceilings. Minor damage such as misalignment was found to occur beyond a maximum acceleration of about 1.5 m/s^2 (0.15g).

Furniture and building contents were damaged at five cases. The main damage was the shift and fall of the shelves that were not fixed. These were damages reported to the facility manager. We could not investigate the damage to tenants, so other damage may have occurred. Figure 6 (c) shows the maximum acceleration at the corresponding floor and the number of damage cases. The monitor installed at a high place fell at 1.0 m/s^2 (0.10g), but it is probable that larger acceleration occurred at the base of the monitor than on the floor. Excluding this case, damage such as fall was found to occur beyond a maximum acceleration of about 3.5 m/s^2 (0.35g). However, it depends on whether measures are taken to prevent falls.

A lot of damage was concentrated around the expansion joints in all four buildings. Large cracks in the partition walls and ceilings around the inter-building connection occurred on each floor, and the expansion joint covers fell out. This is due to the fact that sufficient flexibility was not taken into account at the expansion joint with respect to the different deformation of the connected buildings. On the ninth floor of the damaged building, the maximum relative displacement between the two buildings was 28 mm in the translation direction and 21 mm in the collision direction.

4. Damage estimation of non-structural components

We examined the building response that caused damage to non-structural components. Figure 7 shows damage levels of displacement-sensitive or acceleration-sensitive non-structural components. Here, “no damage” means that non-structural components sustained no damage until the specified displacement or acceleration; “damage” means that at least one non-structural component of the 26 buildings experienced damage in the concerned range; and “uncertain” means that the damage level could not be evaluated because none of the components reached the relevant level of displacement or acceleration. Based on the damage data, a general sequence in which non-structural components are damaged can be estimated such that damage occurred first at expansion joints, followed by interior and partition walls, further followed by ceilings, furniture and building contents, and exterior walls. Doors and window glasses are likely not damaged earlier than other types of non-structural components.

Since we had much damage data for interior partition walls which tended to be damaged even in small interstory drift ratio, we tried to evaluate their fragility curve. Figure 8 illustrates an example fragility curve estimated for interior and partition walls using the data shown in Figure 6 (a). The interstory drift ratio at damage initiation was taken to follow the log-normal distribution. According to this figure, the damage probability exceeds 50% at an interstory drift ratio of 0.13% (1/800). Caution is needed when referring to this curve, because the damage was counted with respect to each floor (i.e., judged damaged if at least one non-structural component was damaged in the floor), and the data was limited for the interstory drift ratio of at most 0.40% (1/250).

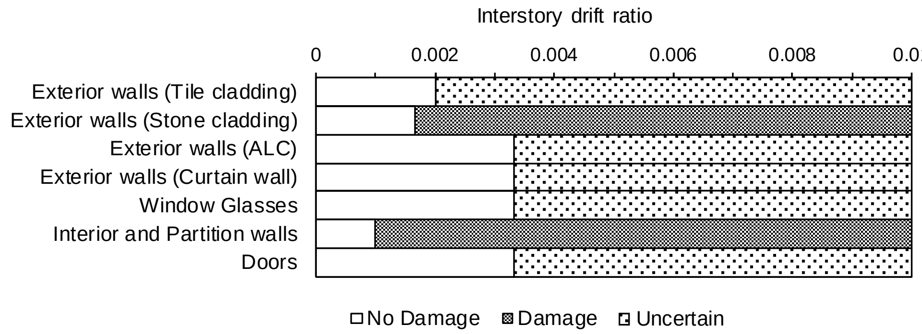

(a)

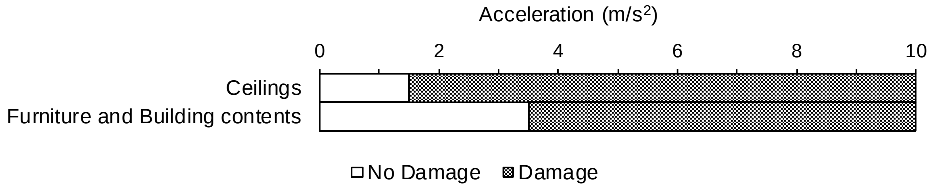

(b)

Fig. 7 – Damage distribution of non-structural components; (a) displacement-sensitive non-structural components with respect to interstory drift ratio; (b) acceleration-sensitive non-structural components with respect to maximum floor acceleration

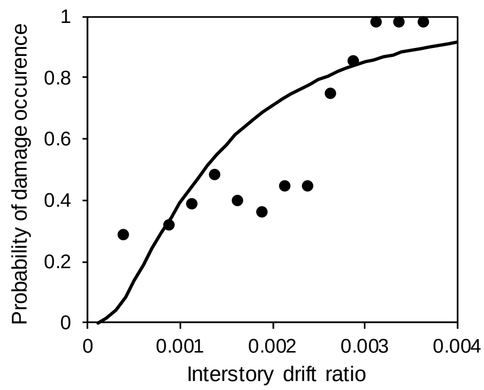

Fig. 8 – Example fragility curve of interior and partition walls obtained from actual damage

5. Conclusions

This paper presents the relationship between damage to non-structural components and the building response. The major findings are listed as follows.

1) A general sequence in which non-structural components are damaged can be estimated such that damage occurred first at expansion joints, followed by interior and partition walls, further followed by ceilings, furniture and building contents, and exterior walls. Doors and window glasses are likely not damaged earlier than other types of non-structural components.

2) As for interior and partition walls, notable damage such as cracks, occurred from a maximum interstory drift ratio of about 0.1% (1/1000).

3) As for ceilings, minor damage such as misalignment occurred beyond a maximum acceleration of about 1.5 m/s^2 (0.15g).

4) An example fragility curve estimated for interior and partition walls was made. According to this fragility curve, the damage probability exceeds 50% at an interstory drift ratio of 0.13% (1/800).

Damage to non-structural components on this earthquake required repair, but there were many minor damages, and the safety limits could not be estimated. However, from the damage investigation to the 26 office buildings installed with sensor, it was found that SHM can effectively facilitate the establishment of fragility curves of a variety of non-structural components. In the future, if a large earthquake occurs, it is possible to update the fragility curve and to improve the accuracy of damage judgement by SHM systems.

6. Acknowledgements

The writers express their sincere gratitude to the building owners and managers who kindly shared the data associated with SHM of the buildings that they own/manage.

7. References

[1] Kambara H, Hayashi Y, Tamura K (2004): Relationship between non-structural elements damage and seismic intensity based on questionnaire survey. *Journal of Structural and Construction Engineering, AIJ*, **578**, 155-161 (in Japanese).

[2] Architectural Institute of Japan (2012): *Proceedings of public workshop on countermeasure of long-period strong motion*, Long-period Building Earthquake Response Subcommittee, Architectural Institute of Japan, 377pp (in Japanese).

